JOURNAL OF MATERIALS SCIENCE 14 (1979) 1914–1922

Fatigue crack initiation in hot isostatically pressed Ti-6Al-4V castings

D. EYLON
Department of Materials Science and Metallurgical Engineering, University of Cincinnati, Cincinnati, Ohio 45221, USA

Precision castings of the Ti–6Al–4V alloy containing pore defects were hot isostatically pressed (HIP) in an attempt to improve the high cycle fatigue strength. Although all defects were healed, the fatigue strength was still low when compared to β-processed wrought material with a similar microstructure. Fatigue-crack initiation analysis, which included precision sectioning, indicated that early fatigue-crack initiation sites were related to relatively large α-platelet colonies and massive grain-boundary α(GBα) phase. Shear across the large colonies or along the GBα interfaces provided large initial cracks which resulted in the fatigue-life degradation. Large colonies and massive GBα developed in the HIP healed zones of the casting pores. In spite of the total HIP pore closure, the fatigue-strength improvement was small when compared to wrought material due to the coarse microstructure that developed in some locations during the HIP cycle. Large planar-shear initiation facets across several colonies were also observed. The multi-colony faceted shear is the result of the Burgers relation between the colony orientations and increases the chance of early fatigue-crack inititation.

1. Introduction

The microstructure of $\alpha+\beta$ titanium alloys cooled from the β-phase region typically consists of α-platelets separated by β-films. The platelets can be arranged either in a basketweave morphology [1] or in packets of similarly aligned and crystallographically oriented platelets called colonies. The α-platelet morphology and the colony size depend on the β-solutioning conditions, the cooling rate, and the amount of β-stabilizing elements in the alloy [2]. The colony structure can be obtained by β-heat-treatment, β-processing or casting. Colonies of various sizes can typically be found in thick sections due to the slower cooling rates.

Crack formation in this morphology is highly dependent on intense slip activity across the colonies [2–4]. Consequently, the monotonic [5] and cyclic [4] loading factures have been shown to be highly microstructurally dependent, leading to relatively high fracture toughness and low crack–propagation rates [3] as compared to $\alpha+\beta$ microstructures which contain equi-axed α-phase. These properties, coupled with inherently good creep resistance [6], make it an acceptable structure for many aerospace applications at low and elevated temperatures, provided the colony size is being kept small [4].

Precision vacuum casting was evaluated [7, 8] in an attempt to produce complex-shaped Ti–6Al–4V components and reduce high machining costs. The cast components exhibited good tensile properties but significantly lower smooth low [7] and high [8] cycle fatigue lives when compared to β-rolled and annealed [9] or β-forged [10, 11] Ti–6Al–4V with similar microstructure. Fig. 1 presents the relatively lower fatigue strength and high data scatter of the cast Ti–6Al–4V [8] when compared to β-rolled plate material with a colony structure [9]. The lower fatigue strength was attributed to a combination of casting defects and highly

 0022–2461/79/081914–09 $02.90/0

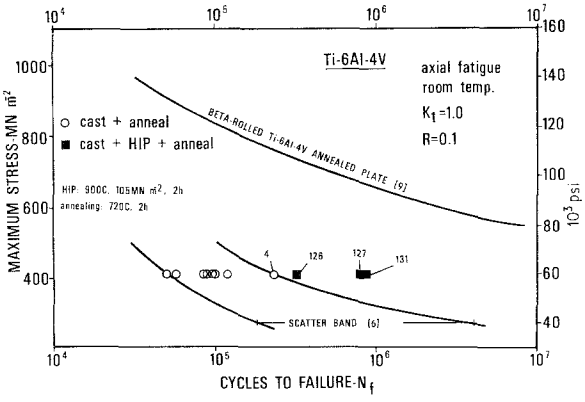

Figure 1 S–N curve for Ti–6Al–4V castings with a wide scatter band and the data points of cast and HIP material without porosity. The S–N curve of β-processed wrought Ti–6Al–4V with similar microstructure is shown for reference.

notch-sensitive colony structure [12] which contributed to crack initiation and failure.

In an attempt to improve the fatigue life, the cast components were hot isostatically pressed (HIP) to close the casting porosity [8]. Although the porosity was healed by the HIP process, the fatigue strength was only marginally improved when compared to typical wrought material (Fig. 1).

Previous studies demonstrated that in defect-free wrought Ti–6Al–4V [13, 14], and other alloys [15], the crack-initiation stage consumed the majority of the high cycle fatigue life. Therefore, investigation of the fatigue-crack initiation stage holds the key to understanding the premature fatigue failures. In this work, the crack-initiation characteristics of cast HIP material were investigated in an attempt to understand the low fatigue strengths.

2. Experimental details

2.1. Material

To enable a valid comparison with previously reported crack initiation analysis of Ti–6Al–4V castings [2], fatigue specimens of cast and HIP material, tested under similar conditions, were selected for examination. Specimens machined from components produced by an investment casting technique [12] were hot isostatically pressed at 900° C and 105 MN m^{-2} for 2 h and were subsequently annealed at 720° C for 2 h. The average room temperature tensile properties of the material were: yield strength = 860 MN m^{-2}, ultimate tensile strength = 965 MN m^{-2}, and elongation (in 4D) = 9% [8]. The chemical composition of the cast material in weight per cent is: 6.2Al, 4.1V, 0.16Fe, 0.02C, 0.0042H, 0.185O, 0.005N, and the balance Ti.

2.2. Microstructure

The cast, HIP and annealed microstructure is shown in Fig. 2a. At the optical microscopy level, it appears that the HIP cycle did very little to change the cast structure of the non-porous areas [12], and the mixture of basketweave structure (A), colony structure (B), and prior beta grain-boundary α (C) remained the same. However, in those locations where large dendritic pores were identified by radiography (Fig. 2c) prior to the HIP cycle, relatively large packet-type colonies (0.3 mm average diameter) and massive grain-boundary α (GBα) which outlines the pre-existing pore, were observed in the post HIP structure (Fig. 2b). The HIP healed zone microstructures were observed by sectioning through the previously identified void locations (Fig. 2c). The extent of the healed zone was determined by low magnification polarized light observation. Fig. 2d is the radiograph of the same porous location in Fig 2c after the HIP cycle and it shows a complete porosity closure. No residual porosity was detected by either radiographic or metallographic techniques in any of the examined HIP specimens. Although HIP was performed below the 995° C transition temperature, the β-annealed structure in the healed zones (Fig. 2b) indicate that these localized areas were cooled from the β-region. This could be the result of either local porosity closure adiabatic heating or local chemical composition changes in the dendritically solidified large pore surfaces [12], which lowered the β-transition temperature.

An energy dispersive X-ray analysis performed by Grisik and Arnold [16], on Ti–6Al–4V castings, showed lower Al content on the pore surface. This can account for lower β-transition temperature; however, quantitative analysis carried

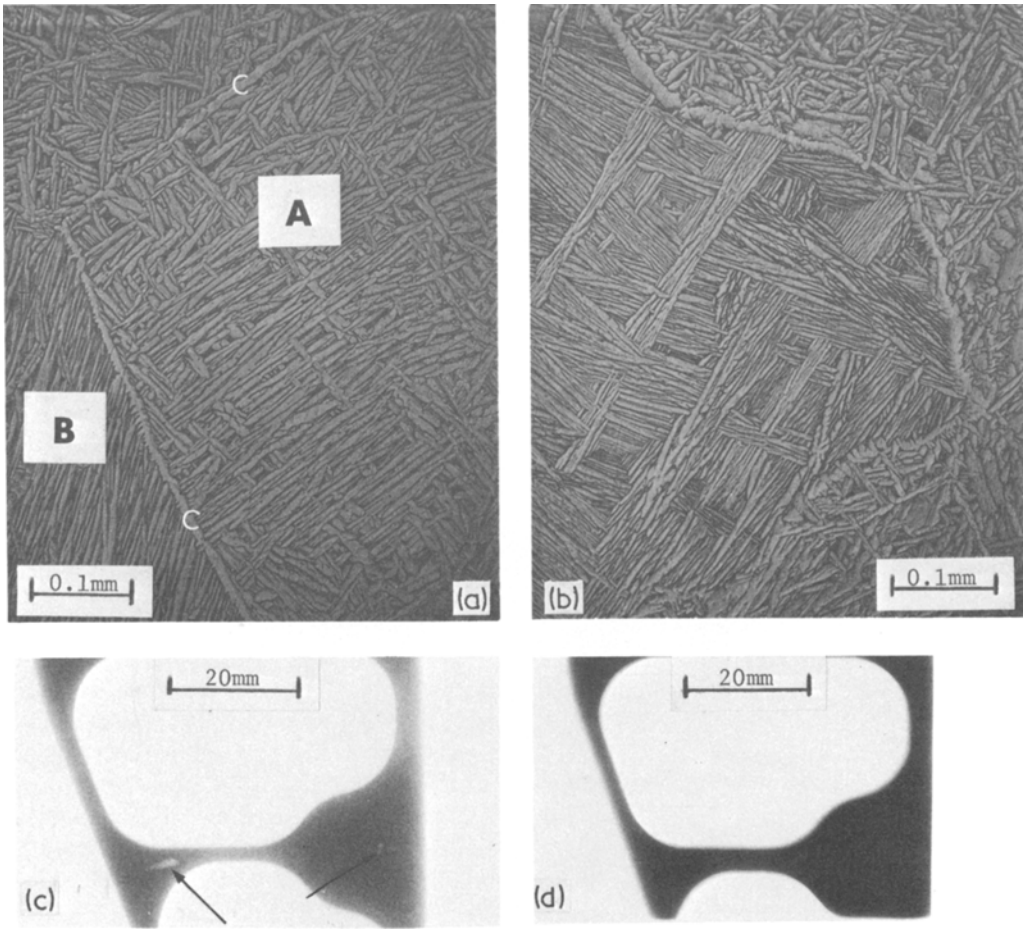

Figure 2 (a) The microstructure of the cast material photographed at a defect-free location, A: basketweave structure; B: colony structure; C: grain-boundary α (GBα). (b) The microstructure of cast and HIP material in a healed pore zone showing colony structure and GBα with the healed zone. The basketweave microstructure is part of the original structure. (c) A radiograph of casting pores in an as cast component segment. (d) A radiograph of the HIP healed segment shown in (c). (b) is taken from the healed zone of the left-hand side pore shown in (c).

out in this work by a similar method, did not show any significant compositional differences between the pore surface and the interior.

2.3. Fatigue tests

Only specimens tested in axial fatigue with a positive stress ratio $R(R = \sigma_{min}/\sigma_{max})$, were examined for fatigue-crack initiation. It was then possible to positively identify and characterize the initiation location since the fracture surfaces were well preserved in the tension/tension loading mode. The flat specimen (10 mm x 2.5 mm gauge cross-section and 25 mm gauge length), were tested at 1800 cycles min^{-1}, room temperature, and $R = +0.1$ [8]. The specimens studied were tested at 414 MN m^{-2} maximum stress level as were the previously reported cast fatigue specimens [12]. The test results are shown in Fig. 1 and Table I.

TABLE I High cycle room temperature axial fatigue tests, $R = 0.1$ [8]

Specimen no.	Maximum cyclic stress (MN m^{-2})	Cycles to failure (N_f)	Initiation	Facet size (mm)
126	414	3.2×10^5	shear-across-colony	0.5
127	414	7.9×10^5	grain-boundary α	0.2
131	414	8.3×10^5	shear-across-colony	0.1

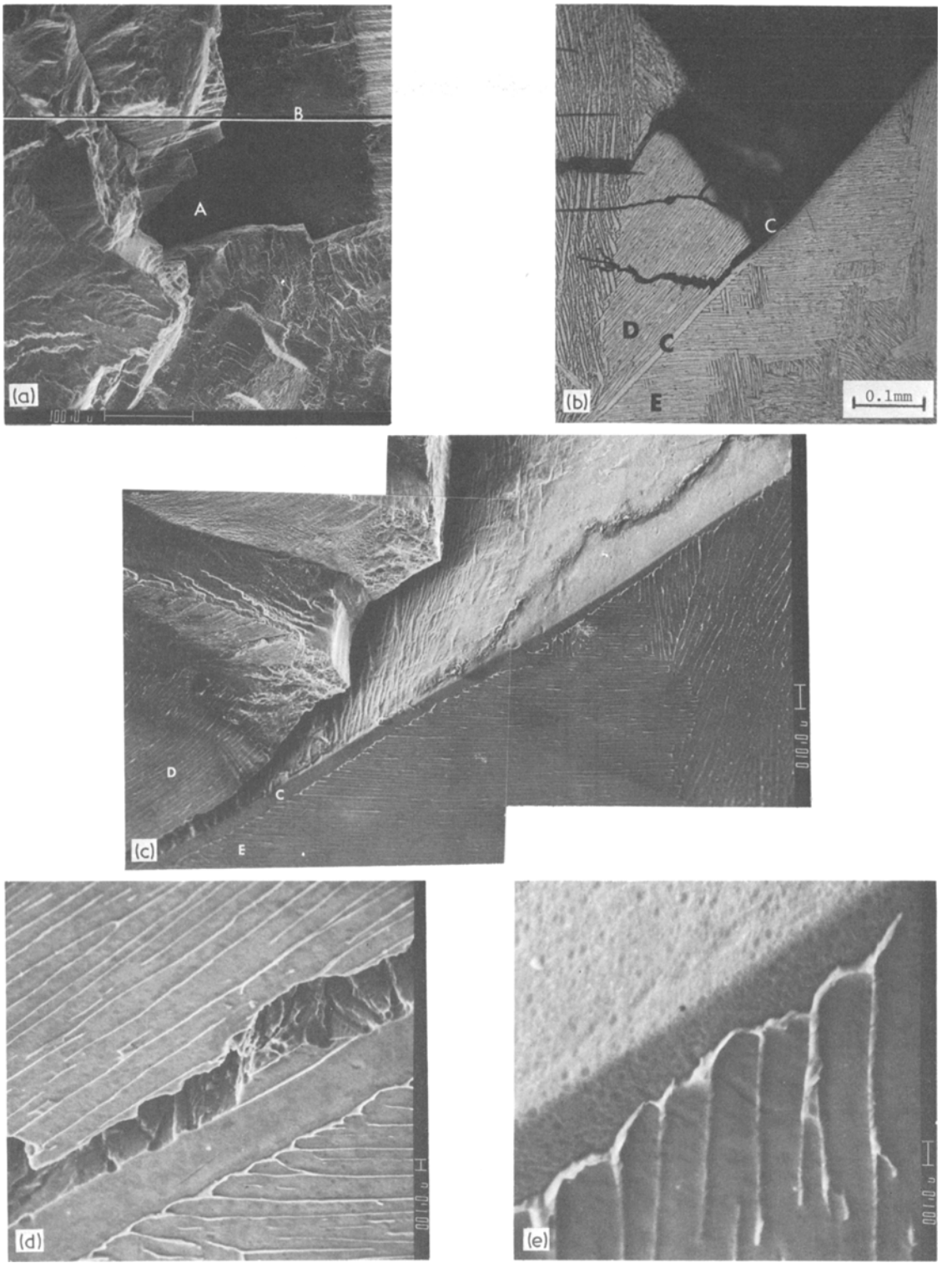

Figure 3 Grain-boundary α fatigue-crack initiation of specimen 127. (a) Fracture initiation facet (A) and section line (B). (b) The section plane and the microstructure under the GBα facet (C) separating colonies D and E. (c) Micrographic/fractographic SEM image of the initiation site at the section plane showing GBα (C) and colonies D and E. (d) High magnification image of the separation zone between the GBα and colony D. (e) High magnification image of the GBα shear zone.

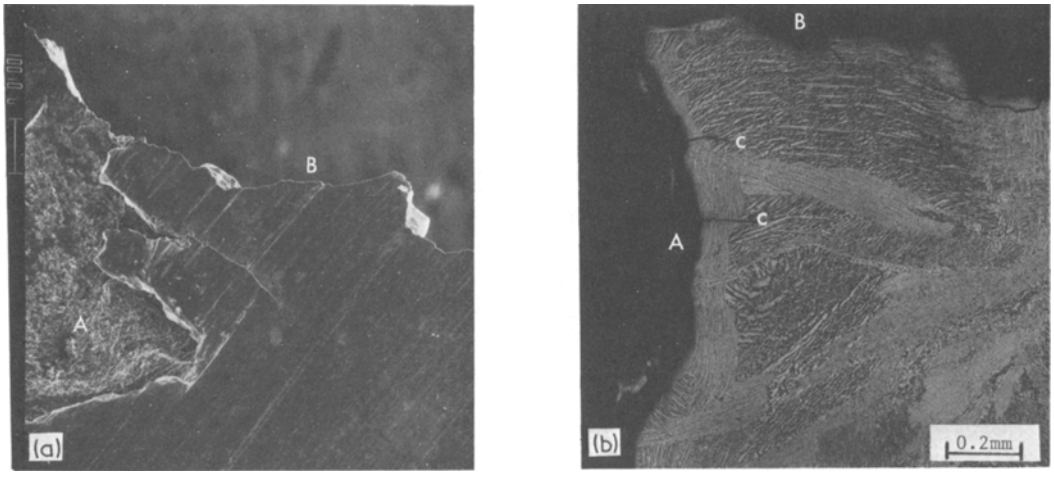

Figure 4 Specimen 127. (a) Large unhealed casting pore (A) on the surface of the specimen, which in spite of its size (1 mm) and its location near the fracture zone, did not initiate the final fracture (B). (b) A section through pore A showing the final fracture B which initiated from the GBα in Fig. 3b. The microcracks C which developed in this region did not grow fast enough to cause the final failure.

2.4. Fractography and precision sectioning

The fatigue-crack initiation sites were identified by scanning electron microscopy using an ETEC scanning electron microprobe. After locating the sites, the specimens were sectioned perpendicular to the fracture surface through the initiation site. The precision sectioning technique is described in detail elsewhere [14]. The sectioned surface was polished and etched with Kroll's reagent and photomicrographs of the initiation location and the underlying microstructure were taken. After optical examination the mounting material was dissolved, making it possible to obtain a combined micrographic/fractographic SEM image of the fracture surface and the initiation site.

3. Crack-initiation analysis

Out of the limited sample of 3 specimens analysed in detail in this work, (Table I), two specimens (nos. 126 and 131) exhibited shear-across-colony initiation, the third (127) had cracks initiated

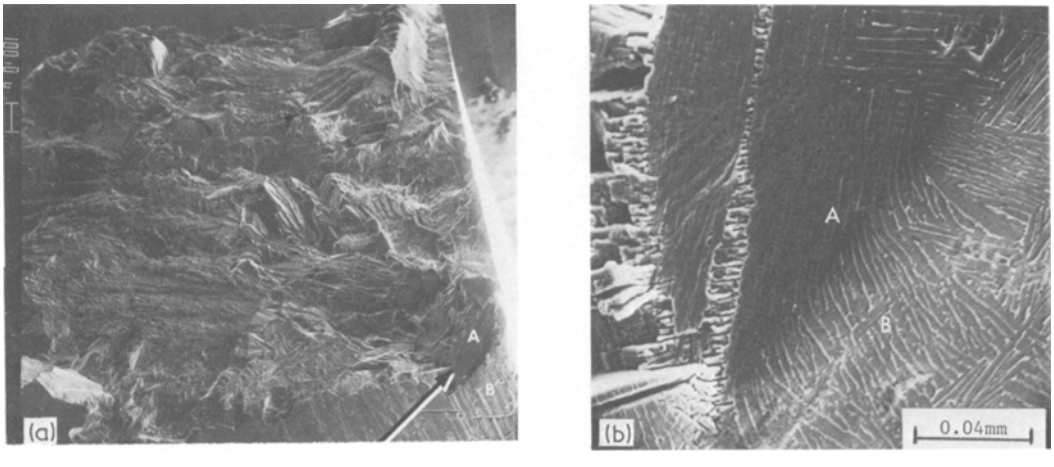

Figure 5 Specimen 131. (a) Shear initiation facet (A) close to the specimen surface (B). The location is marked with an arrow. (b) Section through facet A on plane B shows the microstructure on the etched shear facet A and the underlying microstructure on the section plane B.

along the GBα phase. The specimen numbers correspond to those in the original test report [8] for ease of reference.

3.1. Grain-boundary α (GBα) initiation

The subsurface GBα crack initiation (127) is shown in Fig. 3a and marked A. The specimen was sectioned parallel to line B and the underlying microstructure is shown in Fig. 3b. It can be seen that the initial crack (C) was on the same plane as the GBα, which separates colonies D and E. The tensile axis is in the vertical direction of the photomicrograph. The 45° inclination of the GBα made it a favourable location for crack initiation since it parallels the maximum shear direction. Unlike most GBα in the structure (Fig. 2a and b), this GBα is planar, which also aids crack formation. An angled SEM image which exhibits both the fracture surface and the underlying microstructures in the initiation region is shown in Fig. 3c. The higher magnification image in Fig. 3e shows that the GBα was left intact and that the initial crack occurred along the boundary between the GBα and colony D. Examination of colony D orientation in Fig. 3b and the high magnification image in Fig. 3d shows that the α-platelets were parallel to the GBα plane resulting in the separation on the D side of the GBα. The conditions which made this a favourable initiation site are, therefore:

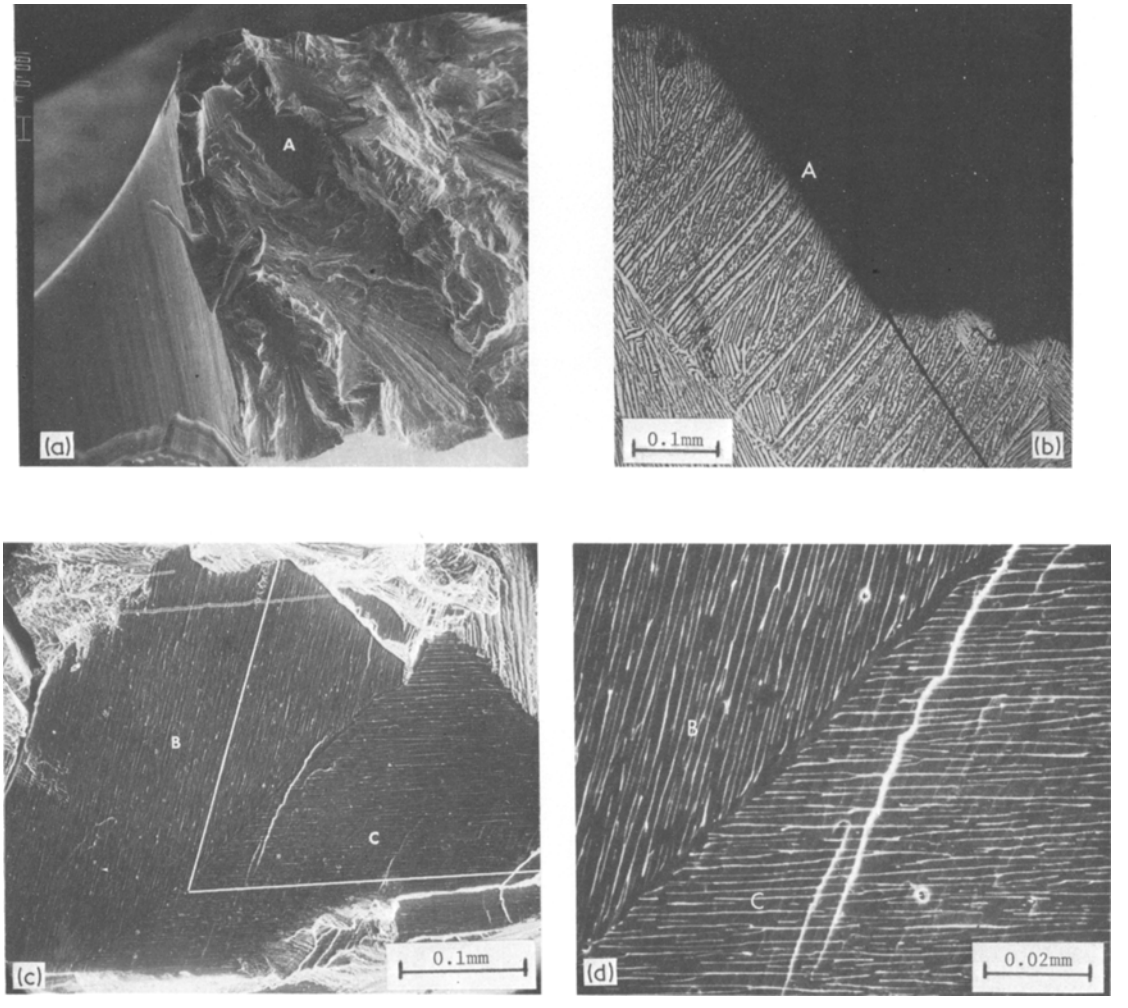

Figure 6 Specimen 126. (a) Large shear initiation facet (A) close to the specimen surface. (b) A section through the facet A showing shear-across-colony initiation. (c) SEM image of the etched facet A showing two colony orientations B and C at a 70.5° angle. (d) High magnification SEM image showing the α/β interface details of colonies B and C along their boundary.

(a) the GBα is planar,

(b) it is inclined at 45° to the tensile direction, and

(c) the α-platelet long axis of the adjacent colony is parallel to the GBα.

Because of the nature of the metal flow in the HIP process, surface porosity cannot be filled and healed. Fig. 4a shows a large surface defect (A) close to the fracture surface (B). In spite of its large size, it did not initiate the terminal crack in specimen 127. A section through this defect (Fig. 4b) reveals a few microcracks (C), none of which matured to final fracture.

3.2. Shear-across-colony initiation

The fatigue failure of specimen 131 initiated from a 0.1 mm shear facet close to the surface and is marked with an arrow in Fig. 5a. A section through the initiation site (Fig. 5b) shows that the shear plane A is inclined to the tensile axis and is almost perpendicular to the long axis of the α-platelets on the section plane (B). The fracture surface was slightly etched with Kroll's reagent to reveal the colony platelet structure.

The initiation site of specimen 126 (Fig. 6a) is similar to 131 (Fig. 5a); however, the shear facet is larger (0.5 mm) and is inclined at 30° to the tensile axis (Fig. 6b). Examination of the mating fracture surfaces showed that there are two colony orientations (B and C) on the facet plane (Fig. 6c). This and the high magnification image in Fig. 6d were photographed from the etched surface of facet A. The facet was accurately placed in the SEM specimen stage so that it was parallel to the image plane, thus enabling the measurement of the angle between the α/β interfaces of the two colonies. The angle is shown in Fig. 6c and was measured to be 70.5°. The surface preparation and the image recording are described in more detail elsewhere [17].

4. Discussion

4.1. Crack-initiation location

Since the HIP operation healed the subsurface porosity, all examined failure initiations were related to microstructural elements rather than to defects. However, the average smooth fatigue life was only marginally improved over that of the porous cast material (Fig. 1). The reason for this minimal improvement is the development of large colonies and massive GBα in the porous locations that were healed by the HIP cycle (Fig. 2). The large colonies [2, 4, 18] and the planar GBα [15] provide favourable locations for shear-related crack initiation. The much higher fatigue lives observed in β-forged Ti–6Al–4V [10, 19] are the result of finer colony structure, the lack of large prior β grains and massive GBα.

Similar GBα initiation was observed in the Ti–17 alloy [15] with similar microstructure that also had planar GBα inclined at 45° to the tensile direction. The large GBα grains are the result of large prior β-grains and slow cooling rates from the β-phase region. The HIP process with its very slow cooling cycle promotes the formation of this phase. In contrast, β-worked and rapidly cooled wrought material would exhibit a structure free of GBα with relatively small colonies and, therefore, better fatigue life.

The shear-across-large-colonies initiation was also shown to reduce drastically the fatigue life in wrought Ti–6Al–4V [14]. The lower fatigue life of IMI–685 [4, 20] was also related to large colony shear. The facet size of specimens 131 and 126 are 0.1 and 0.5 mm, respectively. The lower fatigue life of specimen 126 can be correlated to the shear facet size (Table I). The failure of the cast specimen 4 [12] (Fig. 1) also initiated from a 0.5 mm shear facet.

4.2. Multi-colony faceted fracture

The shear facet of specimen 126 (Fig. 6a) is larger than the average colony size of the healed pore zones (Fig. 2b). The etched surface in Fig. 6c reveals that the shear is across two colonies with a 70.5° trace orientation relationship on the fracture plane. The α-platelet orientation of each colony is related to the prior beta grain (PBG) orientation through one of the 12 possible variants of the Burgers relation [21, 22]:

$$\{1\,1\,0\}_\beta \parallel (0\,0\,0\,1)_\alpha$$

$$\langle 1\,1\,1\rangle_\beta \parallel \langle 1\,1\,\bar{2}\,0\rangle_\alpha.$$

In this case both colonies belong to the same PBG (Fig. 6b) and, therefore, are related through the Burgers relation with the α/β interfaces on or close to the $(1\,0\,1\,0)_\alpha$ prismatic planes [18]. The shear facets in many are on [23] or close [24, 25] to the $(0\,0\,0\,1)_\alpha$ basal plane. 70.5° is a possible angle between the α/β interfaces of two colonies since it

is the angle between the two $[1\,1\,1]_\beta$ which transforms to a $(0\,0\,0\,1)_\alpha$ plane. The 70.5° trace angle, therefore, indicates that the initiation shear facet is on a basal plane. From symmetry considerations [17], 10.5°, 49.5°, and 60° and also possible trace angles on a basal plane fracture, but were not observed in this work. The same multi-colony faceted fatigue fracture was previously observed in wrought β-processed IMI–685, β-annealed Ti–11 [17], and β-processed Ti–6Al–4V [26].

Shear fracture on common plane through more than one colony increases the chance of having shear-initiation facets larger than the colony size and, therefore, lower fatigue life. The probability of multi-colony faceted fracture increases as the PBG size increases [17]. The healed pore areas in the cast and HIP material (Fig. 2b) thus constitute potentially dangerous zones for this type of larger facet initiation.

5. Conclusions

Porous Ti–6Al–4V castings were hot isostatically pressed (HIP) to improve the smooth fatigue life of the material. The HIP process healed the casting pores but based on the limited sample studied here, only moderate fatigue strength increase was observed. Even with this improvement, fatigue strength was still lower than that of wrought products with a similar microstructure. Examination of the failed material shows that:

(1) no residual casting porosity existed in the HIP material;

(2) the HIP healed porous zones produced a large colony and massive grain-boundary α (GBα) microstructure;

(3) Fatigue cracks initiated by (a): shear-across-colony facets, (b): shear-along-GBα facets;

(4) for the same stress level, the shorter fatigue lives were correlated to the larger shear facets;

(5) a planar initiation shear facet across two colonies was observed;

(6) the angular relationship between the α/β interface traces of the two colonies indicates that the facet is on a basal $(0\,0\,0\,1)_\alpha$ plane;

(7) the ability of several colonies within the same prior beta grain (PBG) to shear on the same plane increases the danger of early crack initiation.

Acknowledgements

The author wishes to thank Mr K. Love of the Manufacturing Technology Division, AFML, for his support of this work, and also Mr M. M. Allen and W. T. Barice of Pratt & Whitney and Mr W. Grant of Grumman Aerospace Corporation for providing the material for this work. Mr W.A. Houston of the University of Cincinnati is acknowledged for his assistance in the precision sectioning. Messrs B. Strope and R. A. Bacon of Systems Research Laboratories are acknowledged for performing the scanning electron microscopy. The comments of Dr T.L. Bartel of the Air Force Materials Laboratory and Mr M. Rosenblum of the University of Cincinnati are highly appreciated. The analytical portion of this work was conducted under USAF Contract Number F33615-76-C-5227 and is part of a joint collaborative research effort with the Air Force Materials Laboratory.

References

1. J. C. CHESNUTT, C. G. RHODES and J. C. WILLIAMS, ASTM STP 600 (American Society for Testing and Materials, Philadelphia, PA., 1976) p. 99.
2. D. EYLON and P. J. BANIA, *Met. Trans. A* **9A** (1978) 1273.
3. D. EYLON, J. A. HALL, C. M. PIERCE and D. L. RUCKLE, *ibid* **7A** (1976) 1817.
4. D. EYLON and J. A. HALL, *ibid* **8A** (1977) 981.
5. D. SHECHTMAN and M. J. BLACKBURN, unpublished research (1975).
6. W. M. PARRIS and H. A. RUSSELL, "Titanium Science and Technology", Vol. 4, edited by R. I. Jaffee and H. M. Burte (Plenum, New York, 1973) p. 2219.
7. V. L. HELLMANN and T. C. TSARETT, Air Force Materials Laboratory Report: AFML-TR-71-47, July (1971).
8. W. J. BARICE, M. M. ALLEN and W. GRANT, Air Force Materials Laboratory Report: AFML-TR-76-192, November (1976).
9. F. L. PARKINSON, The Boeing Company Report No. FAA-SS-72-00, July (1972).
10. J. E. COYNE, "The Science, Technology and Application of Titanium", edited by R. I. Jaffee and N. E. Promisel (Pregamon, New York, 1970) p. 97.
11. J. J. LUCAS, "Titanium Science and Technology", Vol. 3, edited by R. I. Jaffee and H. M. Burte (Plenum, New York, 1973) p. 2081.
12. D. EYLON and B. STROPE, *J. Mater. Sci.* **14** (1979) 345.
13. D. EYLON and C. M. PIERCE, *Met. Trans. A* **7A** (1976) 111.
14. W. R. KERR, D. EYLON and J. A. HALL, *ibid* **7A** (1976) 1477.

15. D. EYLON and W. R. KERR, "Fractographic Approach to Failure Analysis", ASTM STP 645 (American Society for Testing and Materials, Philadelphia, PA., 1978) p. 235.
16. J. J. GRISIK and D. B. ARNOLD, Interim Report IR162-2(III) on USAF Contract No. F33615-72-C-1381, Air Force Materials Laboratory, Wright-Patterson AFB, OH 45433, February (1973).
17. D. EYLON, *Met. Trans. A.* **10A** (1979) 311.
18. D. SHECHTMAN and D. EYLON, *ibid* **9A** (1978) 1018.
19. G. T. PETRAK, Air Force Materials Laboratory Report, AFML-TR-70-291, January (1971).
20. D. EYLON, *Microscope* **23** (1975) 133.
21. W. G. BURGERS, *Physica* **1** (1934) 651.
22. J. C. WILLIAMS, "Titanium Science and Technology", edited by R. I. Jaffe and H. M. Burte (Plenum, New York, 1973).
23. D. L. DAVIDSON, ASTM STP 675 (American Society for Testing and Materials, Philadelphia, PA., 1979).
24. D. A. MEYN and G. SANDOZ, *Trans. Met. Soc. AIME* **245** (1969) 1253.
25. D. A. MEYN, *Met. Trans.* **5** (1974) 2405.
26. J. RUPPEN, P. BHOWAL, D. EYLON and A. J. McEVELY, ASTM STP 675 (American Society for Testing and Materials, Philadelphia, PA., 1979).

Received 27 September and accepted 15 December 1978.